

3 Checking validity of the selection function

Abstract

The particle size distribution of fine chemicals in the solid state, like active pharmaceutical ingredients, is often a critical parameter. To achieve the desired particle size distribution, milling of such materials is usually the method of choice. Since these chemicals are often scarcely available, experimental optimization of milling is not possible. Therefore, a model to predict the milling conditions has been developed. The model estimates the rate of breakage function, and needs mechanical properties like hardness and yield strength as input to calculate the rate of breakage function. This paper attempts to check the validity of the model by a series of experiments. A comparison of the experimental results with the outcomes of the model using 5 different model compounds has been performed. It appears that the rate of breakage function can be estimated by:

$$S_i = 5.85(\pm 1.78)10^8 \frac{E_{kin} E_{fract} \sqrt{\frac{P_y}{\rho}}}{V H \sqrt{x_i} K_{1c}}$$

The model is able to rank the compounds in degree of fracture as an effect of milling. It was also possible to perform a quantitative prediction of the impact of milling pressure on the milling behaviour. Finally, it appeared that the prediction of the large particles in the distribution was significantly better than small ones. Because the oversize material is usually the most critical parameter, the conclusion is that the model has acceptable practical applicability.

3.1 Introduction

The particle size distribution of fine chemicals in the solid state like pharmaceutically active materials determines the performance of the final product to a large extent. To obtain the desired specifications milling of these materials is often necessary. It is not possible to predict the required milling conditions only on the basis of particle size distribution of the starting materials, because the mechanical properties of the material influence the milling process too. Generally, experimental optimization of the milling conditions is not an option either, because these types of materials are often scarcely available. Therefore, a theoretic approach towards predicting the best milling conditions is needed. The purpose of this study was to develop a method to predict the desired milling conditions given a specific (organic) solid material. The population balance (1, 2) has been used as a starting point. To reduce the number of tests a model which includes both material and mill properties in the description of particle breakage has been developed (3). This chapter attempts to experimentally check the validity of this model.

3.2 Using the proposed model

The basis in modelling the grinding process is usually a population balance. The population balance describes the correlation between the particle size distribution of the starting material and that of the milled material. Broadbent and Callcott (1) proposed a model of size reduction based on the concept of the rate of breakage function and the breakage distribution function. The rate of breakage function (**S**) is the probability of a particle with a certain size to break per unit time. The breakage distribution function (**B**) describes the size distribution of a particle of given size after fracture. For a discrete size distribution it is convenient to use the model in matrix form (see the nomenclature for a list of symbols) (1):

$$\bar{p} = [\mathbf{S}\mathbf{B} + (\mathbf{I} - \mathbf{S})]^n \bar{f} \quad (1)$$

Provided that milling time is short, Berthiaux and Dodds (2) suggested that the elements of the breakage distribution function matrix can be derived from the elements of the rate of breakage function:

$$b(i, j) = \frac{S_{i-1} - S_i}{S_j} \quad (2)$$

For example, $b(i, j)$ is the fraction product that was originally in size interval j that fell into size interval i after milling. Chapter 2 argued that it is possible to predict the rate of breakage function on the basis of material properties (3):

$$S_i = c \frac{E_{kin} E_{fract} \sqrt{\frac{P_y}{\rho}}}{V H \sqrt{x_i} K_{1c}} \left(\frac{\ell}{x_i} \right) \quad (3)$$

The constant c and the relative length(s) of the initial cracks (ℓ/x_i) are unknown. One of the aims of this chapter is to estimate these values. When this information is available, it is possible to calculate the particle size distribution of the milled material.

For reasons of checking the validity of the method (3), it is also necessary to calculate the rate of breakage function of a material under certain milling conditions on the basis of experiments. For the calculation of the rate of breakage function from the experimental results this chapter uses the approach as suggested by Kapur (4) and following the approach of Berthiaux and Dodds (2) who stated that results can be described using the first-order Kapur function only.

3.3 Materials and methods

3.3.1 Materials

Five different compounds were used. A special sample of coarse α -lactose monohydrate was obtained from DMV (Veghel, The Netherlands), Paracetamol was from BUFA (Uitgeest, The Netherlands). Org 12962 (lot L00018644), a heterocyclic compound A, and Add-Neop which is a steroid (lot L00022481) were all from Diosynth (Oss, The Netherlands). Table 3-1 shows the particle size distributions of the materials before milling.

Table 3-1 Particle size distribution of the materials before milling.

	D(v,10) [μm]	D(v,50) [μm]	D(v,90) [μm]	D(v,99) [μm]
Lactose	68	200	393	560
Compound A	83	256	543	797
Paracetamol	36	139	362	539
Add-neop	26	123	433	702
Org 12962	8	132	408	847

3.3.2 Methods

The milling experiments were performed in a 100 AFG fluidized bed opposed jet mill (Alpine, Augsburg, Germany). This kind of mill is specifically designed for continuous grinding. To perform batch grinding experiments the particle feed was closed and the classifier speed was set to its maximum rotational rate (22000 RPM) to limit the amount of fines leaving the mill chamber. Experiments were performed by placing a given load of powder into the mill and turning the grinding gas on for a defined time period (varying between 20 and 80 s). After milling, the whole content of the mill was removed for particle size analysis using laser diffraction (Malvern Mastersizer S, UK). The particle size

distribution was determined using the Fraunhofer algorithm. The true density of the drug substance was determined with a gas pycnometer (AccuPyc 1330, Micromeritics) using nitrogen as test gas. Data analysis was performed using Mathematica version 4.1.2.0 (Wolfram Research, Champaign, USA, 1988-2000).

3.4 Results and discussion

3.4.1 The correlation between experiments and the prediction

The model materials were ground and Kapur's (4) method was used to determine the rate of breakage functions of the test materials obtained from experimental results, the "experimental rate of breakage functions". Appendix 2 describes the Kapur function in more detail. Figure 3-1 shows the experimental rate of breakage functions of the different compounds. The figure shows that Org 12962 has the highest breakage rate and α -lactose is the compound that shows the lowest fracture rate.

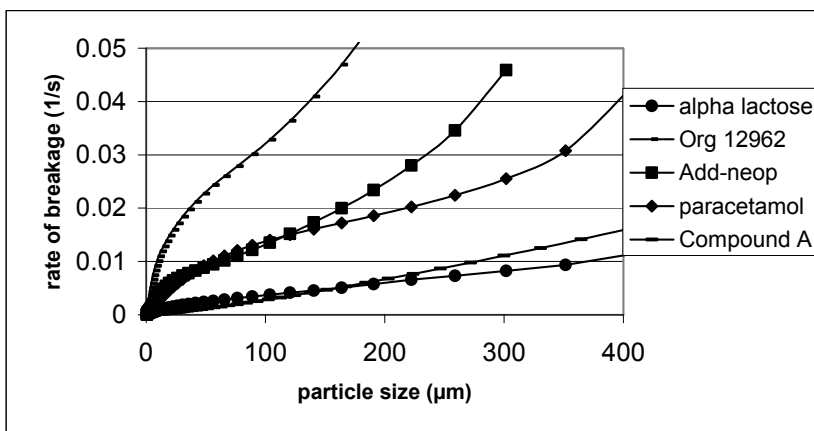


Figure 3-1 Experimentally determined rates of breakage of the compounds.

Chapter 2 showed that it is possible to calculate the rate of breakage function on the basis of a number of material properties and parameters that are correlated with the milling conditions (3). Typical material properties are yield strength and hardness whereas milling pressure and mill chamber volume represents the milling conditions. The equation also contains an unknown dimensionless constant (c) and the relative lengths of flaws (ℓ/x_i), which need to be quantified. Following the approach of Rumpf (5), it is assumed that the fracture in particles of different sizes is similar, i.e. (ℓ/x_i) has a constant value. This implies that the same fracture pattern is present in particles of different sizes. As an effect of this consideration a new dimensionless constant can be defined:

$$k = c \left(\frac{\ell}{x_i} \right) \quad (4)$$

This means that the rate of breakage function becomes:

$$S_i = k S'_i \quad (5)$$

In which S'_i is the “reduced rate of breakage function”:

$$S'_i = \left[\frac{E_{kin} E_{fract} \sqrt{\frac{P_y}{\rho}}}{VH\sqrt{x_i} K_{1c}} \right] \quad (6)$$

Figure 3-2 shows the predicted reduced rates of breakage functions for the five compounds.

The parameters of this rate of breakage function were calculated in chapter 2 (3).

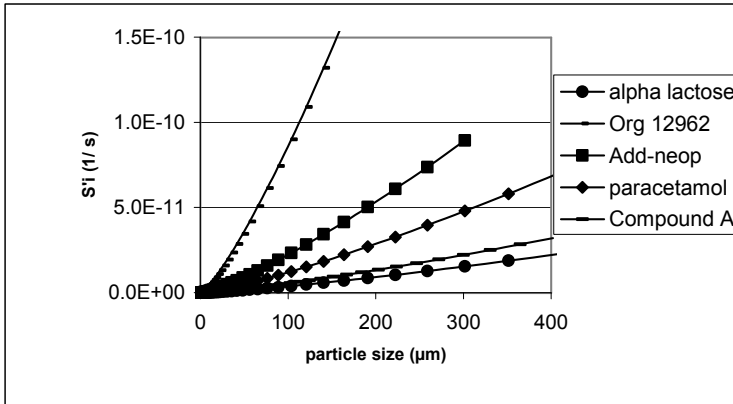


Figure 3-2 Predicted reduced rates of breakage of the model compounds.

Simulated milling pressure is 5 bar (3).

This figure shows that Org 12962 has the highest rate of breakage, whereas lactose shows less fracture. A comparison of the data in Figures 3-1 and 3-2 shows that the rank order of the calculated reduced rates of breakage and experimentally determined values are equal. The conclusion is that the approach allows for differentiation between the milling behaviour of different materials. Furthermore, these data can be used to estimate the dimensionless constant. The dimensionless constant k (eq.5) was determined by plotting the predicted values of the reduced rate of breakage function and the corresponding values of the experimentally determined rate of breakage function (Figure 3-3).

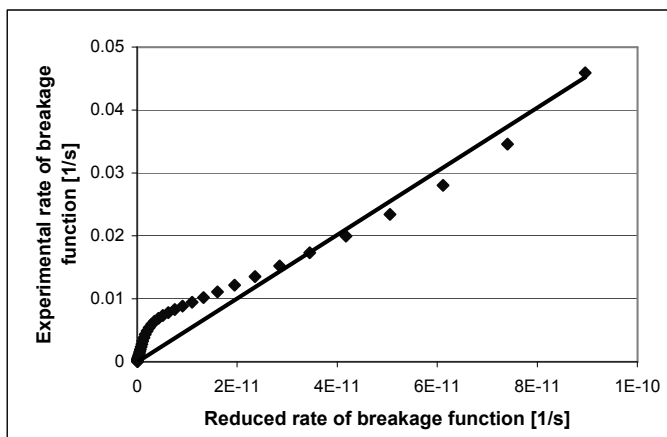


Figure 3-3 Experimental rate of breakage function versus reduced rate of breakage function, together with the linear fit (compound Add Neop).

Linear regression analysis has been performed to calculate the constant k . The regression line was forced through the origin. Figure 3-3 shows that there is strictly no linear relation between the predicted (reduced) rate of breakage function and the experimental rate of breakage function. This aspect will be discussed in section 3.4.2. Linear regression has been performed for all compounds and Table 3-2 shows the dimensionless constants and the 95% confidence intervals.

Table 3-2 Value of the constants as determined with linear regression.

	Constant (k)	Lower 95% limit	Upper 95% limit
Alpha-lactose	$5.79 \cdot 10^8$	$5.49 \cdot 10^8$	$6.10 \cdot 10^8$
Compound A	$7.41 \cdot 10^8$	$7.12 \cdot 10^8$	$7.69 \cdot 10^8$
Paracetamol	$5.76 \cdot 10^8$	$5.32 \cdot 10^8$	$6.20 \cdot 10^8$
Add-neop	$5.05 \cdot 10^8$	$4.70 \cdot 10^8$	$5.39 \cdot 10^8$
Org 12962	$5.24 \cdot 10^8$	$4.84 \cdot 10^8$	$7.69 \cdot 10^8$

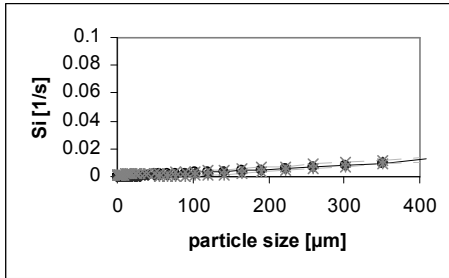
The results in Table 3-2 show that the dimensionless constants are significantly different. This probably can be attributed to the estimation of the parameters needed in eq. 6 for calculation of the reduced rate of breakage function. For example, the theoretical values of particle strength (σ) and stress intensity factor (K_{1c}) are estimated within about 20% of the experimental values (17). Other aspects that play a role are particle morphology and particle velocity. It is assumed that the particle velocity is constant whereas it is reasonable to believe that a velocity distribution profile is present in the mill. All these effects may have a significant impact on the outcome of the calculation of the material properties.

When the assumption is that the model is adequate for the purpose of our application and the differences in Table 3-2 are an effect of errors in estimations of material properties, than it is possible to calculate a mean value of the dimensionless constant. This value is $5.85 (\pm 1.78) \cdot 10^8$. Now, it is possible to simplify the rate of breakage function:

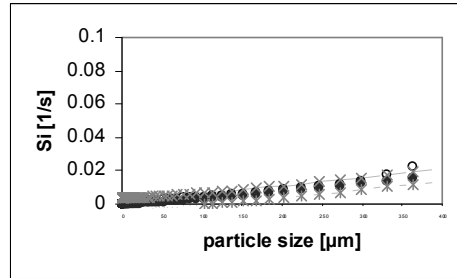
$$S_i = 5.85 (\pm 1.78) 10^8 \frac{E_{kin} E_{fract} \sqrt{\frac{P_y}{\rho}}}{V H \sqrt{x_i} K_{1c}} \quad (7)$$

3.4.2 Accuracy of the prediction

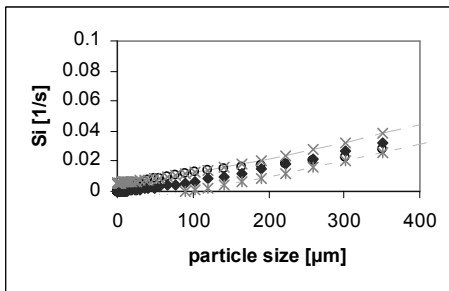
Figure 3-4 compares the predicted rates of breakage (eq. 7) and the measured rates of breakage (Figure 3-1) for each test material.



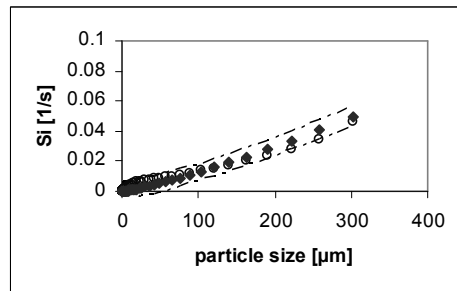
α-lactose monohydrate



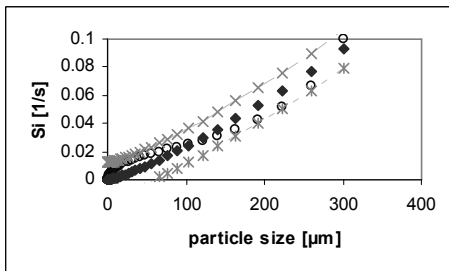
Compound A



Paracetamol



Add-neop



Org 12962

Figure 3-4 Comparison of predicted (\blacklozenge) and experimentally determined (\circ) particle rates of breakage functions of all compounds tested. Constant k is $5.85 \cdot 10^8$. Milling pressure is 5.0 bar. The dashed lines demarcate the 95% confidence interval.

The results show that there is a reasonable correlation between the estimated and predicted rate of breakage function. The materials showing large size reduction (e.g. Org 12962) can be separated from those having less fracture (e.g. lactose). This proves that milling behaviour is

influenced to a great extent by the mechanical properties of the material, because processing conditions for each compound were kept the same.

It is interesting to note that the model under-predicts the degree of fracture when particles are small and there is often an over-prediction when particles are large. This may have several reasons. One of the most important reasons may be that the particle velocity is assumed to have a constant value, whereas it is reasonable to believe that a velocity distribution profile is present in the mill in reality. Following Rumpf (5) it has been assumed that ℓ / x_i is constant. As Rumpf already discussed, in reality this is probably not the case. It is unlikely that 10 times larger particles contain initial flaws that are 10 times larger. The conclusion is that the method has some limitations, but is applicable to determine the starting conditions for milling. Therefore the next step is to predict particle size distributions on the basis of the calculations.

3.4.3 Prediction of the drug substance particle size distribution

The previous section shows that eq. 7 gives an acceptable prediction of the rate of breakage of the different organic compounds used as test materials. In practice the particle size distribution of the milled material is of much more importance. This section compares the predicted and real particle size distributions of the test materials. To predict the product particle size distribution after milling, a simulation was performed using the matrix model of Broadbent and Callcot (1). The product particle size distribution of the ground material (\vec{p}) has been determined with equation 1 (1). Figure 3-5 shows the d_{10} , d_{50} , and the d_{90} of the experimentally determined and the predicted particle size distributions of all compounds, at one operating condition. A comparison of the data shows a reasonable correlation. The deviation at small particle sizes (predominantly d_{10} values) is an effect of the under-prediction of the particle fracture rate when particles are small (see section 3.4.2).

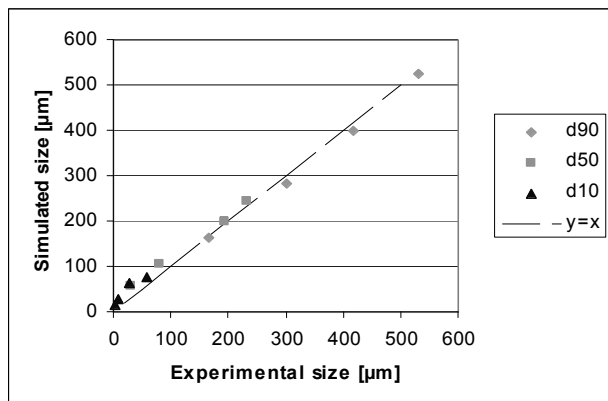


Figure 3-5 The d_{10} , d_{50} and d_{90} values of experimentally determined and predicted particle sizes of all compounds at one operating condition, i.e. 5.0 bar grinding pressure and milling time 40 s.

3.4.4 Extension of milling time

Figure 3-6 shows the predicted and experimentally determined particle size distributions of compound A and lactose after milling. Milling time was 240 s and grinding pressure was 5 bar in both situations. In both cases the predicted and the experimental curves seem to agree reasonably well.

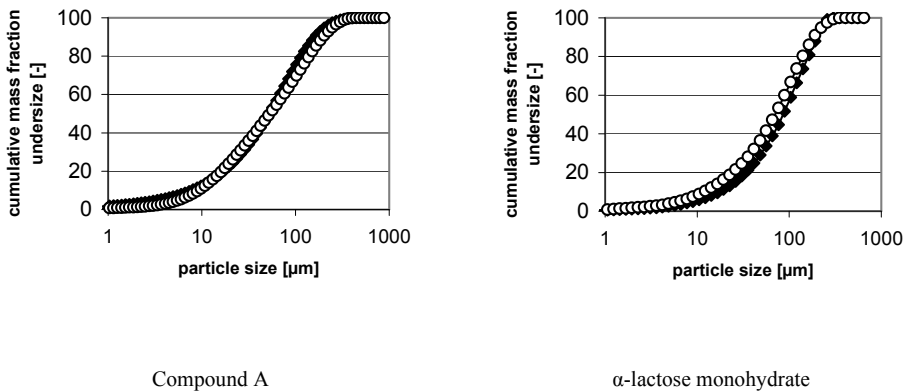


Figure 3-6 Comparison of predicted (◆) and experimentally determined (○) particle size distributions of compound A and α -lactose monohydrate after milling 240 seconds at a milling pressure of 5 bar.

3.4.5 Extension to other milling pressures

Figure 3-7 shows the d_{10} , d_{50} , and the d_{90} values of the experimentally determined and the predicted particle size distributions of lactose, ground at different operating conditions, i.e., 3.5, 4.0, 5.0, and 5.5 bar grinding pressure. Especially, the correlation between the predicted and the experimentally determined d_{50} and d_{90} is good, whereas the correlation between the predicted and the experimentally determined d_{10} is less established. However, since the d_{50} and the d_{90} are often used as a controlling parameter for the particle size distribution, it is concluded that the proposed model seems to be a good description of the milling process.

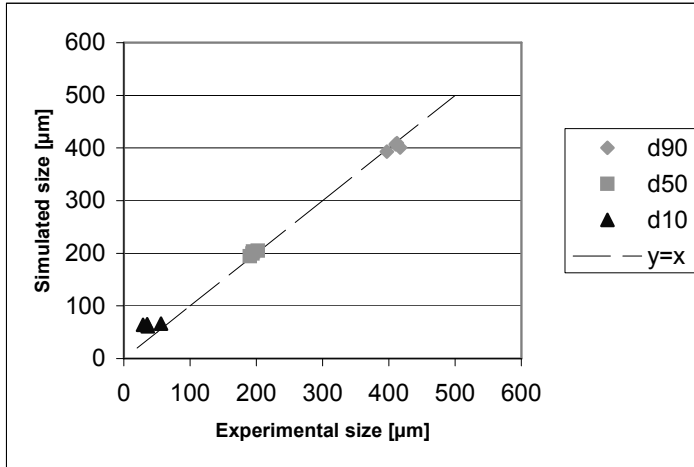


Figure 3-7 The d_{10} , d_{50} and d_{90} values of experimentally determined and the predicted particle size distributions of lactose at different operating conditions, i.e., 3.5, 4.0, 5.0, and 5.5 bar grinding pressure.

3.5 Conclusion

The proposed rate of breakage function in this paper allows the prediction of the rate of breakage function for the materials studied and is reasonably in accordance with experimentally determined values. The rate of breakage for different organic materials can be predicted as follows:

$$S_i = 5.85(\pm 1.78)10^8 \frac{E_{kin} E_{fract} \sqrt{\frac{P_y}{\rho}}}{V H \sqrt{x_i} K_{1c}} \quad (8)$$

The advantage of the method is its simplicity, and the fraction of particles which are reduced in size can be determined quickly for different organic materials. It is concluded that with the proposed method, the particle size distribution after milling can be predicted as well, incorporating process conditions and material properties. As a consequence this will save

quite an amount of scarce material and effort. Furthermore, the method can be used to estimate the particle size distribution in dependence of the milling pressure. This means that a milling pressure can be established beforehand, rather than milling at a standardized pressure.

3.6 Appendix 1: Nomenclature

B	Breakage distribution function	[-]
b_{ij}	Breakage parameter of material going from size interval i to j	[-]
c	Constant	[-]
d_x	Particle diameter where x % of volume of particles is smaller	[m]
E_{fract}	Fracture energy	[J.m ⁻³]
E_{kin}	Kinetic energy of particles	[J]
\vec{f}	Feed vector	[m]
H	Hardness	[Pa]
I	Unit matrix	[-]
$K_i^{(n)}$	Kapur parameter	[s ⁻ⁿ]
K_{1C}	Stress intensity factor	[Pa.m ^{-1/2}]
k	Dimensionless constant	[-]
ℓ	Flaw length	[m]
n	Number of milling intervals	[-]
\vec{p}	Product vector	[m]
P_y	Yield pressure	[Pa]
ρ	Density	[kg.m ⁻³]
$R(t)$	Cumulative fraction retained at time t	[-]
S	Rate of breakage vector	[s ⁻¹]
S_i	Rate of breakage of a particle with size i per time interval	[s ⁻¹]
S'_i	Reduced rate of breakage of a particle with size i per time interval	[s ⁻¹]
V	Volume of mill chamber	[m ³]
x_i	Particle size of fraction i	[m]

3.7 Appendix 2: Kapur function

The experimental particle rate of breakage is determined by means of Kapur's (4) simplification of the batch grinding equation. To apply the method one first has to determine the cumulative fraction oversize $R_i(t)$ with respect to the particle size i at time t . The cumulative fraction oversize $R_i(t)$ is the percentage of particles with a size greater than i . Kapur (4) has shown that the variation of the cumulative fraction oversize $R_i(t)$ can be approximated by equation 8:

$$R_i(t) = R_i(0) \exp \left[K_i^{(1)} t + K_i^{(2)} \frac{t^2}{2} \right] \quad 8$$

where:

$$K_i^{(1)} = -S_i + \sum_{j=1}^{i-1} (S_{j+1} B_{i,j+1} - S_j B_{i,j}) \frac{R_j(0)}{R_i(0)} \quad 9$$

and:

$$K_i^{(2)} = -S_i + \sum_{j=1}^{i-1} (S_{j+1} B_{i,j+1} - S_j B_{i,j}) \left[K_j^{(1)} - K_i^{(1)} \right] \frac{R_j(0)}{R_i(0)} \quad 10$$

The terms K , are called 'Kapur functions' and are functions of the particle rate of breakage function (selection function) and the breakage distribution function. Berthiaux and Dodds (9) demonstrated that the Kapur (4) expression can be reduced to a single term $K_i^{(1)}$ for short grinding times.

3.8 References

1. Broadbent S.R., Callcott T.G., 1956, I: A new analysis of coal breakage processes. *J. Inst. of Fuel* 29, 524-528
2. Berthiaux H., Dodds J., 1996, Approximate calculation of breakage parameters from batch grinding tests. *Chem. Eng. Sci.* 51, 4509-4516.
3. Vegt O.M. de, Vromans H., Faassen F., Voort Maarschalk K. van der, 2005, Milling of organic solids in a jet mill. Part 1: Determination of the selection function and related Mechanical Material Properties. *Part. Part. Syst. Char.* 22, 133 -140
4. Kapur P.C., 1970, Kinetics of batch grinding: Part B. An approximate solution to the grinding equation. *Trans. Soc. Min. Eng. AIME* 247, 309
5. Rumpf H., 1973, Physical aspects of comminution and a new formulation of a law of comminution. *Powder Technol.* 7, 145-159.
6. Roberts R.J., Rowe R.C., York P., 1995, The relationship between the fracture properties, tensile strength and critical stress intensity factor of organic solids and their molecular structure. *Int. J. of Pharm.* 125, 157-162
7. Roberts R.J., Rowe R.C., York P., 1987, The compaction of pharmaceutical and other model materials. *Chemical Engineering Science* 42, 903-911
8. Weichert R., 1991, Theoretical prediction of energy consumption and particle size distribution in grinding and drilling of brittle materials. *Part. Part. Syst. Charact.* 8, 55-62
9. Berthiaux H., Dodds J., 1999, Modelling fine grinding in a fluidized bed opposed jet mill Part 1:Batch grinding kinetics, *Powder Technology* 106, 78-87

